Ultrasonic Induced Material Compression During the Gap-controlled Reshaping of Dry Paper Webs by Embossing or Deep Drawing

André Hofmann,* and Marek Hauptmann

The use of ultrasonic tools in paper forming results in highly dynamic mechanical alternating stress, which causes a changed material load. This work aimed to determine the influence of the ultrasonic process parameters of amplitude, ultrasonic time, and static contact pressure and to characterize the material compression during the ultrasonic-assisted forming of paperboard. To achieve this, a method was developed to determine the static, dynamic, and irreversible material compression during the gap-controlled forming of paper. The results showed that the ultrasonic amplitude, the gap pressure, and their second-order interactions had an important influence on the irreversible material compression. With the new method, the irreversible material compression could be increased up to 480% compared to the equivalent static load case.

Keywords: Paperboard; Ultrasonic; Forming process; Material compression

Contact information: Chair of Processing Machines and Processing Technology, Technische Universität Dresden, Bergstraße 120, 01069 Dresden, Germany;
** Corresponding author: andre.hofmann1@tu-dresden.de*

INTRODUCTION

Paper is a porous material that consists of a network of connected fibers with an anisotropic property profile. In general, it is divided into three main directions, the machine direction (MD), the cross-machine direction (CD), and the thickness direction (ZD). During the paper forming, which is mainly realized through the gap-controlled processes of deep drawing and embossing, paper is stressed by a compressive force in the z-direction (out of plane). In both processes, paper is compressed in the tool gap depending on its ZD-compression behavior and effective process parameters of forming pressure, temperature, and forming time. The basic mechanisms for the compression deformation of paper in the z-direction have been studied in a number of papers (Großmann and Baumgarten 1985; Schaffrath and Götsching 1991; Xia *et al.* 2002; Stenberg 2003; Girlanda *et al.* 2016). According to some researchers' work (Schaffrath and Götsching 1991; Stenberg 2003) the compression of the material leads to a compaction process in which the ratio of pores to fibers is reduced. As a result, the thickness of the material decreases whereas simultaneously the density increases. Some studies show (Stenberg 2003; Nygårds *et al.* 2009 and Girlanda *et al.* 2016) that the increase of the material density leads to a hardening process of the material whereby the compression stiffness increases with the reduction of material thickness. Due to the increase in compressive stiffness, the compression force

exponentially increases with increasing material compression (Stenberg 2002; Girlanda *et al.* 2016).

Researchers (Großmann 1985; Stenberg 2003; Girlanda *et al.* 2016) have found that a viscoelastic and viscoplastic deformation of material occurs during compressive stress, and Großmann (1994) described the elastic deformation proportion as relative compressibility *K*. The relative compressibility *K* governs the relationship between the initial thickness d_a (µm) and the thickness in the compressed state d_r (µm), as written in Eq. 1:

$$\boldsymbol{K}\ (\%) = \frac{\boldsymbol{d_a - d_r}}{\boldsymbol{d_a}} \times \mathbf{100} \quad (1)$$

Consequently, the relative compressibility *K* denotes the irreversible material deformation in the z-direction for the static load case. In addition to irreversible material compression, the elastic compression proportion for the static load case was also described (Großmann 1994). As a result of the compressive stress in the forming process, the thickness is reduced from its initial thickness d_a (µm) by the amount Δd_{stat} (µm). After the material has been stressed, the compression proportion *K* is reduced by the amount *R* (elastic proportion). Only the irreversible proportion *K* (%) of the compression remains in the material.

Girlanda *et al.* (2016) attributed this to the elastic behavior of the material, which leads to a time-dependent recovery of the material. Großmann mentioned the time-dependent material recovery as a relative recovery *R* (Großmann 1994) that can be determined using Eq. 2, where d_r (µm) is the material thickness after recovery:

$$\boldsymbol{R}\ (\%) = \frac{\boldsymbol{d_r - d_k}}{\boldsymbol{d_a - d_r}} \times \mathbf{100} \quad (2)$$

With the above-described mathematical correlations (1) and (2), the basic compression behavior of paper in the z-direction for conventional forming processes without ultrasonic vibrations is represented. The stress in the z-direction has been investigated in converting processes, such as calendaring, in various research studies (Chapman and Peel 1969; Gratton and Crotogino 1988). Furthermore, Stenberg (2003) and Borgqvist *et al.* (2015) presented the analytical model approaches to describe the mechanical behavior of paper in the z-direction. The models enable the simulation of the elastic-plastic behavior for compressive stress in the z-direction, as they occur during the creasing process.

The use of ultrasonic-supported tools in paper converting processes has led to technological improvement, which also affects the compression process of paperboard. Recent studies about the use of ultrasonic vibrations in paper processing have shown the positive effects on increasing surface smoothness while maintaining material volume (Wanske 2010) and also on rapid material heating and compression during deep drawing of paper (Löwe *et al.* 2017). Wanske (2010) and Löwe *et al.* (2017) reported that the material is heated up in the tool gap as a function of the ultrasonic parameters, such as amplitude *A* (µm), ultrasonic time (t_{US}, s) , and static contact pressure (p_{stat}, MPa). Löwe *et al.* (2017) attributed this to the compressive cyclic stresses in materials as a result of the ultrasonic vibrations. Simultaneously, these oscillating compressive stresses in the z-direction in the tool gap result in a large increase in material compression. The influence of the ultrasonic technology on the compression process of paperboard in the tool gap is shown in Fig. 1.

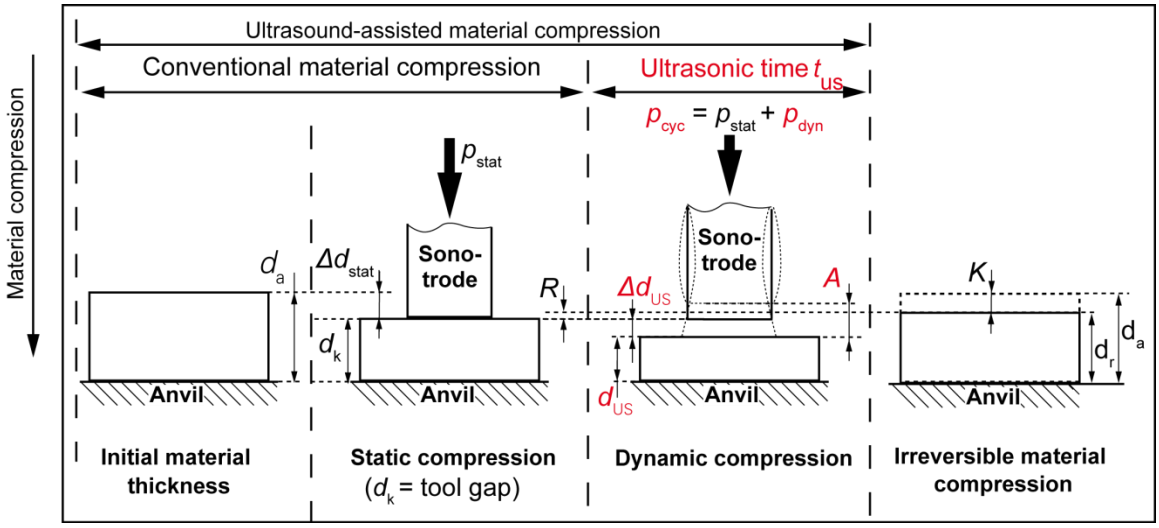

Fig. 1. Simplified illustration with force and compression parameters for conventional and ultrasonic-assisted material compression of paperboard

In the first step, the tool gap between the sonotrode and the anvil is adjusted. Depending on the compression properties of the used paperboard, the static contact pressure (p_{stat}) and the material thickness (d_k) are adjusted, where d_k corresponds to the tool gap between sonotrode and anvil. With the initiation of ultrasonic oscillations, the upper tool (sonotrode) was deflected from its rest position by half magnitude of the amplitude (A, µm). Due to deflection, the material was stressed with a cyclic pressure (p_{cyc}, MPa) that was obtained from the sum of the p_{stat} and the dynamic pressure (p_{dyn}), and then produced a further dynamic material compression (Δd_{US}, µm). The irreversible dynamic material compression (K_{US}, %) and the elastic dynamic material compression (R_{US}, %) can be calculated with the following Eqs. 3 and 4:

$$\boldsymbol{K_{US}}\ (\%) = \frac{\boldsymbol{d_k - dr_{US}}}{\boldsymbol{d_k}} \times \mathbf{100} \quad (3)$$

$$\boldsymbol{R_{US}}(\%) = \frac{\boldsymbol{d_{rUS} - d_{US}}}{\boldsymbol{d_k - d_{rUS}}} \times \mathbf{100} \quad (4)$$

This results in totally irreversible compression K_t for the ultrasonic-assisted forming process according to the following Eqs. 5:

$$\boldsymbol{K_t}\ (\%) = (\boldsymbol{K} + \boldsymbol{K_{US}}) - (\boldsymbol{R} + \boldsymbol{R_{US}}) \quad (5)$$

Currently, there are no studies or equations about the influence of ultrasound on material compression in the z-direction. However, by intensifying the material compression of dry paper webs by ultrasonic vibrations, the process for the production of 3-dimensional packaging by deep drawing can be improved, because a comparatively high compression of the wrinkles can occur in the drawing gap. This can, for instance, improve the dimensional stability and the pressure stability of the 3D molded parts. Simultaneously, the results also provide an important contribution to the refinement of paper by *e.g.* embossing. The embossing motif or the embossing process can be improved by the increased material compression due to the ultrasonic vibrations.

Therefore, this work focused on studying the connections between the ultrasonic parameters, the material compression in the gap-controlled shaping processes for deep-drawing or embossing of dry paper webs. A further goal was to characterize the ultrasonic-dependent magnitude of the irreversible material compression.

EXPERIMENTAL

Materials

All of the experiments were performed at 23 ± 1 °C with an air humidity of 50 ± 2%. Before the tests, the materials were climatically conditioned for at least 24 hours to ensure a moisture balance between the surrounding environment and the material. The material was a three-layered fresh fiber paperboard Trayforma Natura (Stora Enso, Imatra, Finland) with a grammage of 350 g/m² and a material thickness of 450 ± 2 µm. The used paperboard Trayforma Natura was a material from a single production batch.

Test Equipment

To execute the experiments, a laboratory system shown in Fig. 2 was developed.

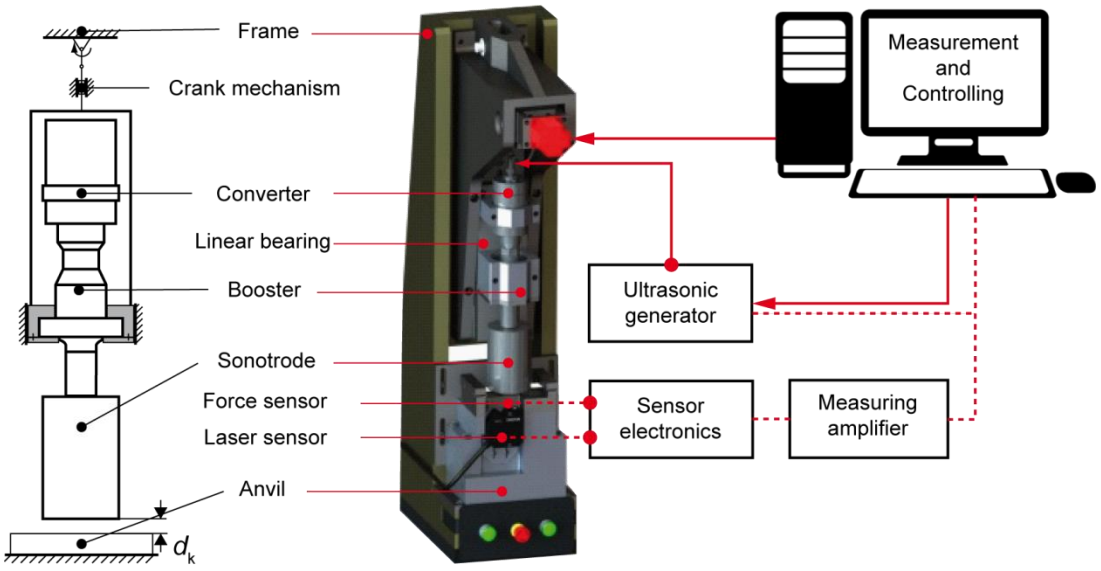

Fig. 2. Illustration of the laboratory system for the investigation of the dynamic material compression in the gap-controlled ultrasonic-assisted forming of paperboard

The device was equipped with a 20 kHz oscillation system (Herrmann Ultraschall, Karlsbad, Germany) and a bar sonotrode with a diameter of 65 mm. The maximum electrical power of the ultrasonic generator (Herrmann Ultraschall, Karlsbad, Germany) was 4300 W. A maximum amplitude of 30 ± 1 µm was realized with the ultrasonic devices used. The tool gap between the bar sonotrode and anvil was adjusted using a servo-mechanically driven crank mechanism. In the stretched position of the crank mechanism, the transmission links form a vertical line, whereby high stiffness is achieved. To ensure a constant static tool gap during the ultrasonic process, the ultrasonic process was performed in the stretching position of the crank mechanism. During the embossing process, a

constant distance between the sonotrode and anvil was ensured, whereby the tool distance in the ultrasonic process was defined by the distance between the rest position of the sonotrode and the anvil surface.

The detection of the static and dynamic force components in the ultrasonic process was achieved using a quartz crystal force sensor (Kistler 9213B; Kistler, Winterthur, Switzerland) positioned in the power flow. The force sensor had a resolution of 0.01 N for real-time measurements in the range up to 2500 N. In combination with the Kistler sensor a charge amplifier (type 5015A; Kistler, Winterthur, Switzerland) guaranteed a sampling rate of 1 MHz, which enabled the force signal of the ultrasonic process to be sufficiently reproduced. The determination of the oscillation amplitude was accomplished using a triangulation laser sensor (LK-H52; Keyence Corporation, Osaka, Japan) with a sampling rate of 390,000 Hz and a resolution of 1 µm. With a statistically verified determination of the dynamic material compression, the process pressure and the ultrasonic amplitude were recorded with a sampling rate of 1000 kHz. With an ultrasonic frequency of 20 kHz, there were 50 measured values per vibration cycle. Due to technical boundary conditions of the measuring computer, the amount of process data recorded during the ultrasonic process led to a critical utilization of the computer's memory, which limited the measurable ultrasonic time to 1000 ms.

In the investigation on the forming of paperboard, the gap-acting static contact pressure (p_{stat}) was adjusted by the tool gap between the sonotrode and anvil listed in Table1. The static contact pressure (p_{stat}) simulates the material-specific compression resistance in the tool gap. As a result of the static contact pressure, the material was subjected to compression. The level of the static compression was determined by the amount of contact pressure. Through adjusting the static contact pressure, the ultrasound was activated. During the ultrasonic treatment, the gap was held constant. A summary of the parameter settings for the investigation of the influence of ultrasonic tools on the material compression in the z-direction is given in Table 1.

Table 1. Parameter Levels for the Experiments

Parameter	Settings										Effect Test Matrix	
											(-)	(+)
Static contact pressure (p_{stat}, MPa)	0.1		0.5		2		2				0.5	2
Tool gap (d_k, µm)	390		270		205		205				270	205
Ultrasonic amplitude (A, µm)	0	5	10		15	20	25	30			5	30
Ultrasonic time (t_{US},sec)	0.15				0.5		1				0.15	1

The compression present in the material after the ultrasonic-assisted forming was determined using a Frank thickness gauge following DIN EN ISO 534 (2012). The K_{US} (%) was determined based on the material-specific compression stress curve and the continuous recording of the static contact pressure. The change in contact pressure in the tool gap also changed the thickness of the material. The mathematical connection between the change of material thickness and the change of contact pressure in the tool gap was determined by the compressive stress curve in Fig. 3a. The real-time force signal can be used to determine the material thickness as a function of the processing time.

Figure 3b shows a typical pressure curve as a function of the processing time that occurred in the investigation. With the adjustment of the tool gap, a static contact pressure was generated depending on the compression resistance of the paperboard. By this means,

a smaller tool gap led to a high static contact pressure. With the ultrasonic activation, an additional dynamic pressure was introduced into the material, which resulted in a reduction of the material thickness in the tool gap and consequently in a drop in the pressure signal. In this paper, the effective pressure after the ultrasonic duration was described as ultrasonic pressure (p_{use}). As already mentioned, the pressure drop correlated with the reduction of material thickness in the tool gap. Consequently, part of the dynamic material compression resulted from the difference of p_{stat} (MPa) after adjusting the tool gap and p_{use} (MPa) at the end of the ultrasonic time. Using the relationship between material compression and effective compression pressure shown in Fig. 3a, the material thickness in the tool gap was calculated at the beginning and end of the ultrasonic treatment. The difference between the two calculated values represents the proportion of the dynamic material compression as a result of the ultrasonic treatment.

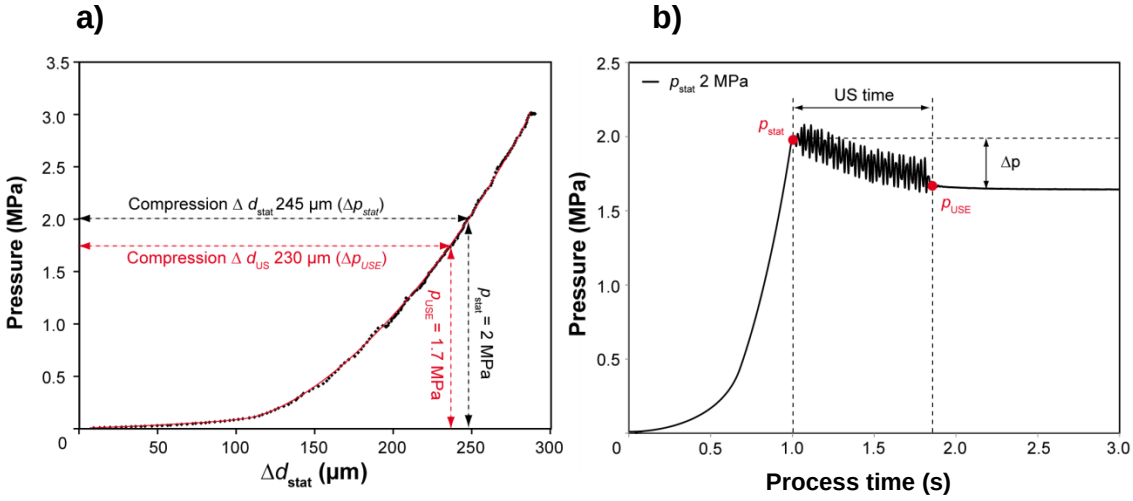

Fig. 3. Typical pressure-compression curve for compression in the z-direction (a) and the process-pressure curve for ultrasonic-assisted compression of paperboard (b) on the example of the Trayforma Natura 350

With the used material and the described experimental setup, ratios of the ultrasonic amplitude (A) to the material thickness in the tool gap d_k ranging from 0.1 to 25% were studied for their influence on the material compression.

Statistical Methods

To obtain information about the influence of the process parameters and their interactions on the dynamic material compression, a full factorial experimental design was prepared. The influence of the adjustable process parameters on the change of the material compression in the z-direction is understood as an effect. The individual effects and interactions were determined using statistical methods of multiple regressions. The test matrix used to determine the effects contained three factors (ultrasonic amplitude, ultrasonic time, and static contact pressure) (Table 1). This resulted in 8 test points that were repeated 10 times to ensure statistically safe results. Thus, the dimensionless parameter effects were calculated from the difference between the response matrix (y_i) of the upper ($x_{i(+1)}$) and the lower ($x_{i(-1)}$) parameter level using Eq. 4:

$$Effect = \frac{\sum_{i=1}^{n} y_{i(+)}}{n_{y_{i(+)}}} - \frac{\sum_{i=1}^{n} y_{i(-)}}{n_{y_{i(-)}}} \quad (5)$$

The parameter levels (-) and (+) used for the effect calculation are described in Table 1. Based on the results calculated from Eq. 3, a standardized effect diagram was generated that contained the individual effects and the noticeable second- and third-order interactions. The assessment of the systematic difference between the empirically and normally distributed determined mean values $y_{i(+)}$ and $y_{i(-)}$ was carried out using the independent sample t-test. The statistical significance of the individual effects and their interactions was tested using the P-value for the calculated effect and the determined significance level of 5% (α=0.05). For the investigations, the calculated effect was statistically significant if the P-value was smaller than the selected significance level α.

RESULTS AND DISCUSSION

As a result of the static contact pressure, the material was subject to a compression K. The amount of K_{stat} was determined by the pressure compression curve (Fig. 3a). The application of mechanical vibrations to the material caused an additional dynamic material compression of the pore volume as a result of the dynamic pressure. The effect of the adjustable process parameters (ultrasonic amplitude, ultrasonic time, and static contact pressure) on the K and the K_{US} were determined based on the parameter levels (+) and (-) of the effect test matrix by multiple regression. Figure 4 shows the standardized effect diagram of the adjustable process parameters and their interaction on K and K_{US} in the gap-controlled forming process.

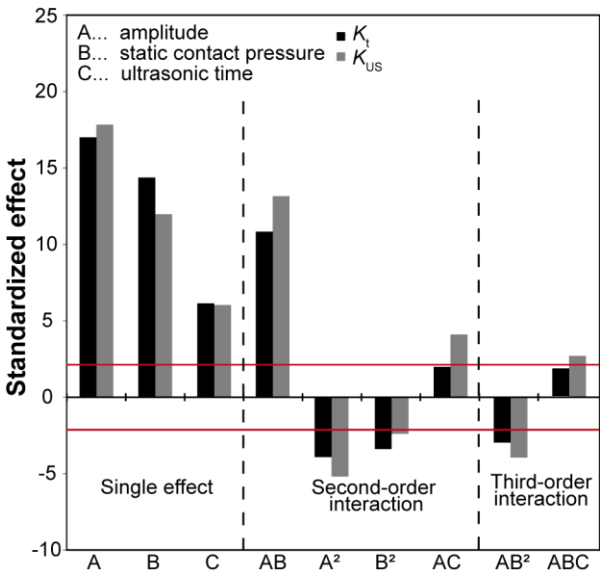

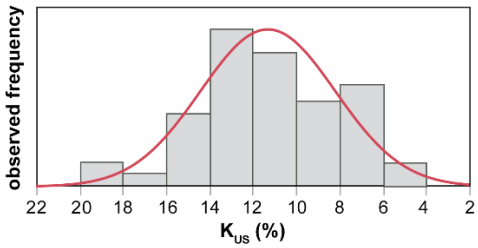

Effect	T-value	P-value
A	17,69	<0,001
B	12,62	<0,001
C	6,69	<0,001
AB	14,73	<0,001
A²	-5,05	0,0098
B²	-2,51	0,0431
AC	4,02	0,0249
AB²	-3,34	0,0379
ABC	2,63	0,0791

Fig. 4. Standardized effect diagram and statistical key figures for K_{US}

The irreversible material compression represents the remaining material compression after the material relaxes and was determined using a thickness gauge. The amplitude and the static contact pressure greatly influenced the dynamic as well as the irreversible material compression (Fig. 4), which can be seen from the large positive single and quadratic second-order interactions of the amplitude and the static contact pressure.

Figure 5a shows the dependence of K_{US} on p_{stat} at different ultrasonic amplitudes. The positive effect of the static contact pressure on K_{US} results from the ratio of the material

thickness to the adjusted tool gap. In general, compared to the material thickness, a smaller tool gap produced a higher static process pressure or contact pressure. Consequently, high static contact pressures resulted in a smaller tool gap in which the effects of ultrasonic vibration achieved a greater dynamic compression effect. In this context, the high effect of the second-order interaction between the amplitude and the static contact pressure in the tool gap was also explained. With the increase of the static contact pressure, the ratio of the ultrasonic amplitude to the tool gap or material thickness also increased. Compared to lower static contact pressures, higher static contact pressures created a higher dynamic pressure as a consequence of the effective ultrasonic amplitude, which gave rise to a larger reduction of the pore volume in the fiber network.

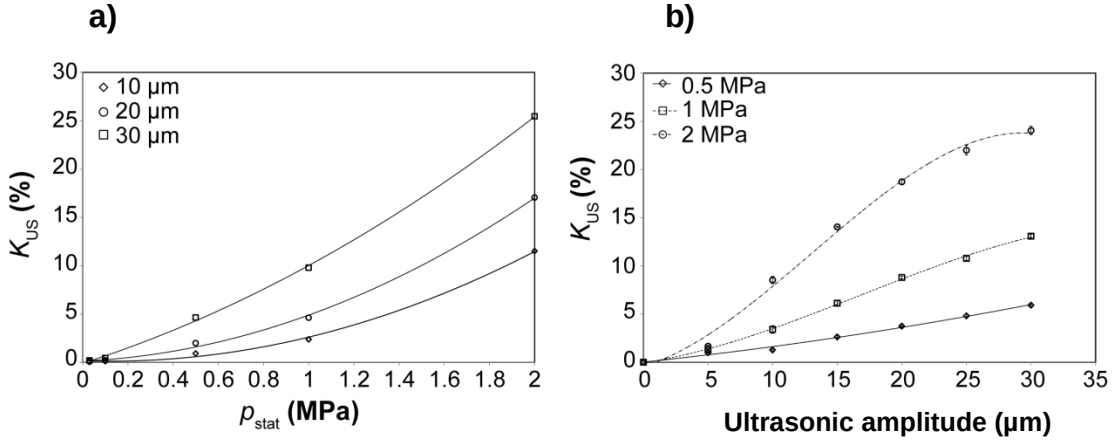

Fig. 5. Dynamic material compression as a function of the static contact pressure (a) and the ultrasonic amplitude (b) for Trayforma Natura 350 g/m²

As mentioned above, another major process variable besides the contact pressure is the ultrasonic amplitude. With the increase of the ultrasonic amplitude, the mechanical deflection in the sonotrode also increased. As a result, the dynamic pressure increased. Greater ultrasonic amplitude generated greater alternating pressure stress in the fiber network, whereby the compression of the fiber network increased with the amplitude. The quadratic influence of the ultrasonic amplitude and the static contact pressure illustrated in Fig. 4 was a result of the non-linear compression behavior of paperboard. According to some publications (Großmann 1985; Stenberg 2003; Nygårds *et al.* 2009; Girlanda *et al.* 2016), a nearly linear increase in material compression has been observed for low compressive stresses. As the material compression increases, the pore volume in the paper decreases. A lower pore volume produced a high compression resistance of the paper with comparatively low material compression in the z-direction, whereby the compression resistance increased in a quadratic manner compared to the material compression. The quadratic increase of the compression resistance was achieved up to a material compression without air inclusions in the paper, the so-called zero point of pore volume. The compression of the paperboard beyond zero point of the pore volume resulted in a lot of fiber damage (Großmann 1985). Therefore, the non-destructive material compression converges against a material-specific threshold, which is why a negative quadratic connection results during the ultrasonic-assisted material compression process analogous to the classical force-deformation process of paperboard. The described effect of amplitude on K_{US} is shown in Fig. 5b. In the range of low p_{stat} up to 1 MPa, a linear correlation between the ultrasonic amplitude and K_{US} was observed. At a p_{stat} of 2 MPa, a plateau was formed

within the range of 20 to 30 µm high ultrasonic amplitudes. The increase of the amplitude from 25 µm to 30 µm did not create a large increase in the dynamic material compression. Therefore, higher material compression is only possible by increasing the static contact pressure.

In relation to the ultrasonic amplitude and the static contact pressure, the ultrasonic time also represented an important factor for K_{US}. However, the influence of latter factor was smaller compared to the previous two factors. Compared to the ultrasonic amplitude and the static contact pressure, the ultrasonic time did not influence the amount of p_{dyn}, which mainly influences K_{US}. The ultrasonic time was used to control the amount of ultrasonic work done on the paper. By increasing the ultrasonic time, the ultrasonic amplitude has a longer lasting impact on the material, which increases K_{US} of the paperboard. In comparison to the p_{stat} and the ultrasonic amplitude, a negative quadratic influence was theoretically observed at high ultrasonic times, which was caused by the gap-controlled forming process. A material compression was only possible up to a material-specific threshold, which resulted from the ratio of tool gap to ultrasonic amplitude. As soon as this threshold was reached, K_{US} could not be increased by a longer ultrasonic time, in contrast to force-controlled compression processes where the tool is tracked and thus the compressive stress remains almost constant during the process. For the amplitudes of 10 µm in Fig. 6a, the material-specific threshold of K_{US} was outside of the maximum ultrasound time of 1000 ms. At a p_{stat} of 1 MPa and an amplitude of 30 µm, this material-specific threshold was reached after approximately 400 ms by the formation of a plateau (Fig. 6b). Further ultrasound treatment did not lead to any further change in K_{US}.

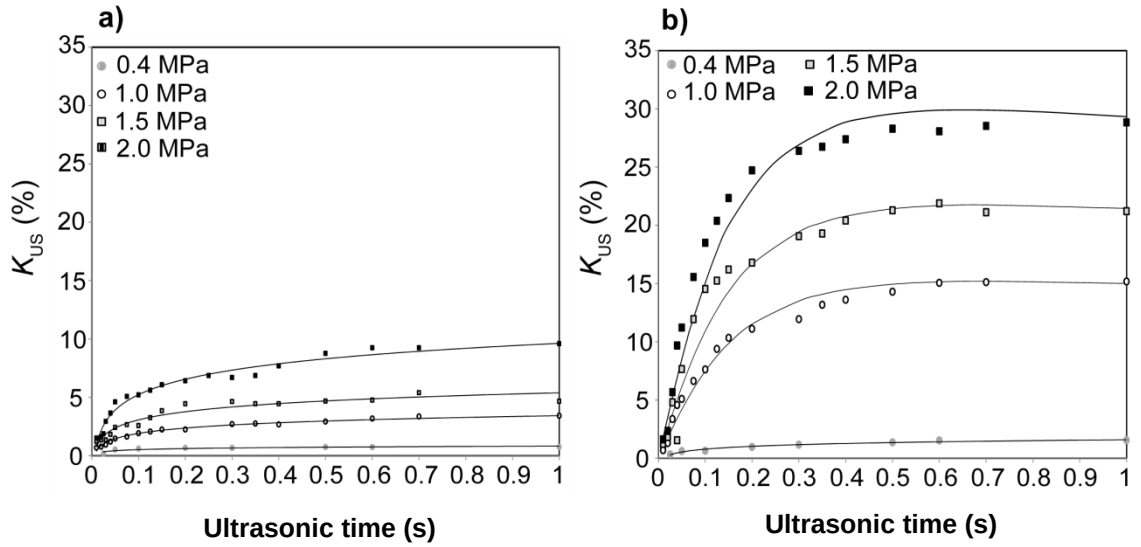

Fig. 6. Influence of the ultrasonic time and static contact pressure on the dynamic material compression for the ultrasonic amplitudes 10 µm (a) and 30 µm (b)

In addition to K_{US}, the ultrasonic parameters also influenced K. To determine the influence of the ultrasonic parameters on the K, the material was treated with 3 static contact pressures and different amplitudes ranging from 0 to 30 µm, as well as an ultrasonic time of 1 s.

Figure 7 shows the compression potential of the ultrasonic-assisted material compression compared to the static load case. It was obvious that the change of K_{US} due to ultrasonic vibrations led to a noticeable increase of K. As described earlier, K_{US} increased

with the ultrasonic amplitude. At the same time, this led to an increase in *K*. For a p_{stat} of 0.5 MPa and an ultrasonic amplitude of 30 µm, a 2.8 times higher *K* was achieved. With the increase of the static contact pressure up to 2 MPa, the effect of the ultrasonic amplitude on the dynamic and irreversible material compression both increased. For ultrasonic amplitudes of 30 µm, a 4.8 times higher *K* was achieved compared to the static pressure of 2 MPa.

Generally, the investigations showed that the observance of the temporal regime of the climatic conditioning of the samples had a considerable influence on the dynamic material compression. Short climatic conditioning times caused a lower material moisture content, which seemed to have a negative effect on material compression. However, the influence of material moisture content on the material compression was not investigated in the context of this work. It should be the subject of further investigations concerning a possible industrial exploitation of the results.

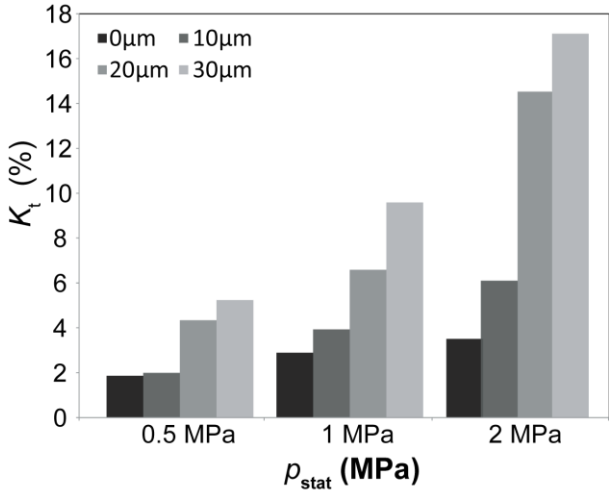

Fig. 7. Comparison of *K* in conventional and ultrasonic-assisted gap-controlled compression processes of paperboard as a function of amplitude

The irreversible material compaction was noticeably influenced by the dynamic material compression or the ultrasonic process parameters (amplitude, ultrasonic time, and static contact pressure). The general connection between dynamic and irreversible material compression is shown in Fig. 8a. Between dynamic and irreversible material compression a quadratic connection can be observed. Determination of the irreversible material compression was made after the sample was unloaded using a thickness gauge. According to Stenberg (2003), Hauptmann (2010), and Girlanda *et al.* (2016), after the compression process, a material-specific recovery occurs as a result of material relaxation and the elastic deformation portion. As the material strain increases, the proportion of elastic deformation also increases (Stenberg 2003). It was assumed that the quadratic connection between *K* and K_{US} resulted from the elastic deformation portion that increased with the compression load. Girlanda *et al.* (2016) reported that the cyclical compression of paper in the z-direction leads to hardening or an increase in compressive stiffness as a function of the number of compression cycles and the deformation amplitude. As a result, the E-modulus and thus the elastic deformation portion increase with each pressure cycle. In the ultrasonic-assisted forming of paper, the material is stressed with approximately 20000 pressure cycles/s. Due to the described effect of material hardening, the R_{US} increased with the K_{US} (Fig. 8b).

Furthermore, after Haslach (2000) and Schmied *et al*. (2013) a creep effect occurred during the static load, which increased with the load duration and thus led to a decrease of p_{stat} during the material compression process. Similar to the cyclic humidification of paper under constant load by Salmén *et al.* (2018), ultrasonic-assisted compression resulted in a high number of dynamic load cycles with short load durations, which increased the creep effect and favored the quadratic relationship between K_t and K_{US}. For the determination of K and R in the static load case, the samples were relieved immediately after reaching p_{stat}, whereby the effect of creep had no noticeable effect on the results of K and R. The calculated values for K_{US} and R_{US} depend on the compression resistance of the material and were directly influenced by creep. According to Salmén *et al.* (2018), a high load duration with alternating load cycles resulted in high creep rates. High creep rates led to an increase in K_{US} combined with a reduction in R_{US}. Especially at high ultrasonic amplitudes and ultrasonic durations there should be an increase of K_{US}. However, Fig. 6b shows that there was no further change in K_{US} for an ultrasonic duration larger than 500ms. Due to the comparatively short maximum ultrasonic duration of 1 second and the low maximum static loads of 2 MPa, the creep effect showed no noticeable influence on the compression values K_{US} and R_{US} in the ultrasonic process despite the high number of load cycles. Therefore, the creep effect was regarded as negligible in the discussion of the results for K_{US}, $R_{US,}$ and K_t.

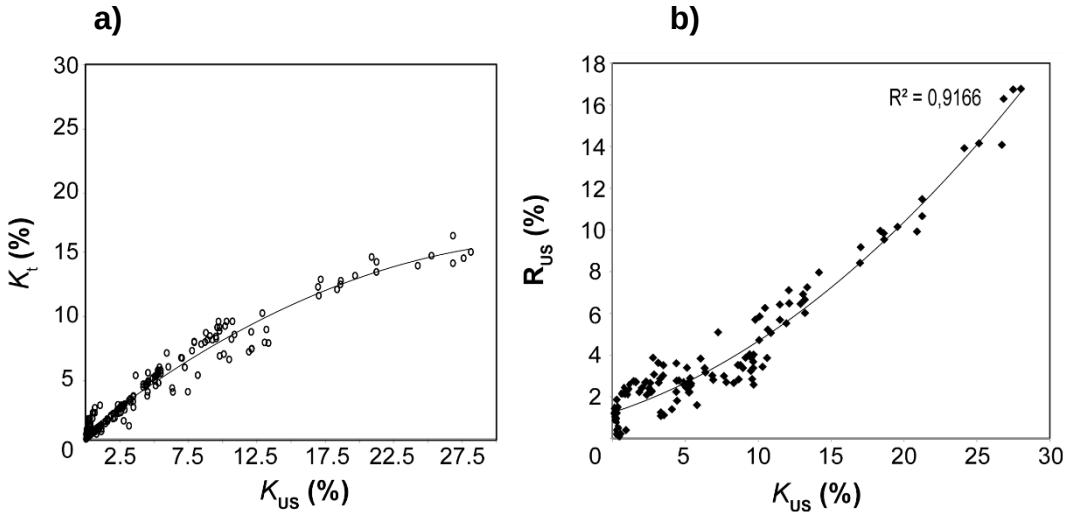

Fig. 8. (a) Connection between K_{US} and K_t and (b) R_{US}

CONCLUSIONS

1. Test equipment and methods were presented to characterize the material compression during the ultrasonic-assisted forming of paper work. The method can be used to determine the universal connection between the dynamic and the irreversible material compression and the process parameters of gap-controlled paper forming. The determined connections between the ultrasonic parameters and the material compression in the z-direction can be applied easily to other paper materials.
2. The effect of the ultrasonic vibrations in the forming process caused a sharp drop in the static contact pressure within 200 milliseconds. This effect can be attributed to ultrasound-induced irreversible dynamic compression.

3. The ultrasonic treatment of the used material with static contact pressure of 2 MPa and an ultrasonic amplitude of 30 µm resulted in a 480 % increase in K compared to the static load case in the conventional forming process.
4. The magnitude of K_{US} is mainly determined by the quadratic relationship to p_{stat} and the ultrasonic amplitude. The irreversible dynamic compression increased with the increase of the ultrasonic amplitude and p_{stat}. As a result of the strong ultrasonic vibrations (p_{stat} = 2 MPa and A =30 µm), up to a 30% increase in K_{US} was achieved.
5. When K_{US} increased, so did R_{US}. The elastic recovery and the irreversible dynamic material compression were characterized by a quadratic relationship, which is why there was an exponential relationship between K_{US} and K.
6. The proportion of the ultrasonically induced K_{US} can be controlled by the ultrasonic amplitude as well as the ultrasonic time. Regardless of the ultrasound amplitude, no noticeable increase of the K_{US} was observed after an ultrasonic time of approximately 0.4 s.

ACKNOWLEDGMENTS

The authors greatly acknowledge the support of the German Federation of Industrial Research Association (AiF) and the German Federal Ministry for Economic Affairs and Energy (BMWi) through the funding of the research project 19717 BR.

REFERENCES CITED

Borgqvist, E., Wallin, M., Ristinmaa, M., and Tryding, J. (2015). "An anisotropic in-plane and out-of-plane elasto-plastic continuum model for paperboard," *Composite Structures* 126, 184-195. DOI: 10.1016/j.compstruct.2015.02.067

Chapman, D. L., and Peel, J. D. (1969). "Calendering processes and the compressibility of paper (Part1)," *Paper Technology* 10(2), 116-124.

DIN EN ISO 534:2012-02 (2012). "Paper and board - Determination of thickness, density and specific volume," International Organisation for Standardization, Berlin, Germany

Girlanda, O., Tjahjanto, D. D., Östlund, S., and Schmidt, L. E. (2016). "On the transient out-of-plane behaviour of high-density cellulose-based fibre mats," *Journal of Material Science* 51(17), 8131-8138. DOI: 10.10007/s10853-016-0083-5

Gratton, M. F., and Crotogino, R. H. (1988). "The effect of Z-direction mositure gradient and temperature gradients in calendering of newsprint," *Journal of Pulp and Paper Science* 14(4), 82-90.

Großmann, H. (1994). *Verfahrenstechnische Grundlagen Der Papierherstellung* [*Procedural Basics of Papermaking*], PTS, München, Heidenau.

Großmann, H., and Baumgarten, H. L. (1985). "Zum Verhalten von Papier und Karton in der Kompressionsphase des Messerschnittes" [Behavior of paper and cardboard in the compression phase of the blade cut] *Das Papier* 10(A), 74–88.

Großmann, V. (1985). *Untersuchungen zum Verarbeitungsverhalten von Karton Beim Rillen mit Bandstahlschnittwerkzeugen [Investigations on the Processing Behaviour*

of Cardboard When Grooving With Steel Strip Cutting Tools], Doctoral Thesis, Technical University of Dresden, Dresden, Germany.

Hauptmann, M. (2010). *Die Gezielte Prozessführung und Möglichkeiten zur Prozessüberwachung Beim Mehrdimensionalen Umformen von Karton durch Ziehen [Targeted Processes Control and Possibilities for Process Monitoring in Multidimensional Reshaping of Cardboard by Pulling]*, Doctoral Thesis, Technical University of Dresden, Dresden, Germany.

Löwe, A., Hofmann, A., and Hauptmann, M. (2017). "The use and application of ultrasonic vibrations in the 3D deformation of paper and cardboard," *Journal of Materials Processing Technology* 240, 23-32. DOI: 10.1016/j.jmatprotec.2016.09.006

Nygårds, M., Just, M., and Tryding, J. (2009). "Experimental and numerical studies of creasing of paperboard," *International Journal of Solids and Structures* 46(11-12), 2493-2505. DOI: 10.1016/j.ijsolstr.2009.02.014

Schaffrath, H. J., and Götsching, L. (1991). "The behaviour of paper under compression in z-direction," in: *TAPPI - International Paper Physics Conference Proceedings*, Kona, Hawaii, USA,

Stenberg, N. (2002). *On the Out-of-Plane Mechanical Behaviour of Paper Materials*, Doctoral Thesis, Royal Institue of Technology Stockholm, Stockholm, Sweden.

Stenberg, N. (2003). "A model for the through-thickness elastic – plastic behaviour of paper," *International Journal of Solids and Structures* 40(26), 7483-7498. DOI: 10.1016/j.ijsolstr.2003.09.003

Wanske, M. (2010). *Hochleistungs-Ultraschallanwendungen in Der Papierindustrie: Methoden zur Volumenschonenden Glättung von Oberflächen [High-performance Ultrasonic Applications in the Paper Industry: Methods for Volume-saving Smoothing of Surfaces]*, Doctoral Thesis, Technical University of Dresden, Dresden, Germany.

Xia, Q. S., Boyce, M. C., and Parks, D. M. (2002). "A constitutive model for the anisotropic elastic – plastic deformation of paper and paperboard," *International Journal of Solids and Structures* 39(15), 4053–4071. DOI: 10.1016/S0020-7683(02)00238-X

Article submitted: July 2, 2019; Peer review completed: September 7, 2019; Revised version received: January 28, 2020; Accepted: January 31, 2020; Published: February 10, 2020.
DOI: 10.15376/biores.15.2.2326-2338